Optical characterizations of heavily doped *p*-type $Al_xGa_{1-x}As$ and GaAs epitaxial films at terahertz frequencies

Z. G. Hu, M. B. M. Rinzan, S. G. Matsik, and A. G. U. Perera[a)]
Department of Physics and Astronomy, Georgia State University, Atlanta, Georgia 30303

G. Von Winckel, A. Stintz, and S. Krishna
Center for High Technology Materials, Electrical Engineering and Computer Engineering (EECE) Department, University of New Mexico, Albuquerque, New Mexico 87106

(Received 10 December 2004; accepted 25 February 2005; published online 27 April 2005)

The optical properties of *p*-type $Al_xGa_{1-x}As$ ($x=0$, 0.01, and 0.16) epitaxial films with different beryllium and carbon doping concentrations ($10^{18}-10^{19}$ cm^{-3}) were investigated by far-infrared reflectance spectroscopy in the 1.5–15-THz frequency range. The dielectric response functions of the film samples were expressed using the classical Lorentz–Drude model. Optical properties were obtained using a three-phase model (air/film/substrate) which agrees with the experimental reflectance spectral data. The effects of doping concentrations on the optical constants were studied in detail. The results indicate that the refractive index increases with the doping concentration in the low-frequency region ($\leqslant 5$ THz) where the free-carrier absorption plays an important role in the optical response. However, the extinction coefficient increases with the doping concentration in the entire frequency region. This indicates that the absorption coefficient increases with the doping concentration. The calculated plasma frequencies agree with the values obtained from the measured doping concentrations. The free-carrier scattering time is $\sim 1.39\times 10^{-14}$ s. The longitudinal-optical phonon plasmon coupled modes of the $Al_xGa_{1-x}As$ films are presented. The upper coupled mode increases with the doping concentration and shows a transition from phononlike to plasmonlike behavior. A sublinear relationship between the absorption coefficient and the doping concentration for *p*-type $Al_xGa_{1-x}As$ epitaxial films was obtained at a frequency of 3.75 THz (80 μm). These results can be used to design and improve the performance of terahertz detectors. © *2005 American Institute of Physics*. [DOI: 10.1063/1.1894581]

I. INTRODUCTION

In recent years, with the breakthroughs in III-V epitaxial growth techniques, GaAs and $Al_xGa_{1-x}As$ thin films have found wide applications in optoelectronic devices. One of the important applications of the $Al_xGa_{1-x}As$ films is in terahertz detectors (i.e., far-infrared detectors: 1 THz=300 μm).[1–4] High-performance heterojunction and homojunction interfacial work-function internal photoemission (HEIWIP and HIWIP) terahertz detectors have stimulated further interest on the terahertz optical properties of the $Al_xGa_{1-x}As$ films. The detection mechanism of HEIWIP and HIWIP terahertz detectors involves free-carrier absorption in the heavily doped emitter layers, followed by the internal photoemission of photoexcited carriers across the junction barrier and then collection by the contact. Therefore, the free-carrier absorption studies can be used to improve HEIWIP and HIWIP performances in the terahertz frequency region.[5]

The far-infrared (FIR) or the terahertz measurements on materials are of great importance due to the phonon frequency and optical constants that can be found in the region.[6,7] The terahertz optical properties of the $Al_xGa_{1-x}As$ film materials are interesting since the free-carrier absorption plays an important role in the detector applications. The free-carrier optical properties of GaAs with carrier concentrations up to 2×10^{18} cm^{-3} can be reasonably described with the Drude model as suggested by Huggard *et al.*[8] It was shown recently that the Drude model is valid for the silicon layers with carrier concentrations up to 3×10^{19} cm^{-3}.[9] This work will focus on the reasonability of the Drude model for heavily doped $Al_xGa_{1-x}As$ films. The optical constants (i.e., the refractive index and extinction coefficient) of semiconductor materials are important in the device design and analysis. It is also of scientific interest to obtain the analytical expression for the optical response of semiconductors.[10] The optical constants of $Al_xGa_{1-x}As$ materials have been reported previously for intrinsic and/or *n*-type bulk materials and films with Al fraction *x* greater than 0.20 beyond the 3-THz frequency.[11] The absorption of the terahertz detectors depends not only on the absorption coefficient (through the extinction coefficient) but also on the refractive index. Therefore, the optical constants are important for calculating the FIR absorption of the terahertz detectors.[2] This makes it important to study the optical constants of materials in the lower-frequency region, where the reststrahlen absorption band is absent and the free-carrier effects become dominant.

The longitudinal-optical phonon plasmon (LPP)-coupled modes can be directly studied using infrared reflectance spectra.[12] Although there are some reports on the LPP-coupled modes of *p*-type $Al_xGa_{1-x}As$ films using Raman scattering,[13,14] the LPP-coupled modes were not well analyzed for the high hole concentrations in the infrared reflec-

[a)]Electronic mail: uperera@gsu.edu

tance spectral measurements.[15] The upper LPP-coupled mode has not been observed in Raman scattering for *p*-type GaAs materials due to a higher damping constant, higher hole effective mass, and lower hole mobility.[16,17] Therefore, the infrared reflectance spectra could be a suitable tool to study the LPP-coupled modes for *p*-type $Al_xGa_{1-x}As$ films.

Here, the optical properties of *p*-type $Al_xGa_{1-x}As$ ($x=0-0.16$) epitaxial films with different beryllium (Be) and carbon (C) doping concentrations are reported using FIR reflectance spectroscopy. The effects of the doping concentration on the optical constants and LPP-coupled modes were investigated.

II. EXPERIMENT DETAILS

Two sets of *p*-type $Al_xGa_{1-x}As$ film samples were grown by molecular-beam epitaxy (MBE) at a growth temperature of 550 °C. The first set of four samples was 1-μm-thick Be-doped epitaxial $Al_xGa_{1-x}As$ ($x=0.01$ and 0.16) films grown on a 520-μm-thick semi-insulating GaAs(100) substrate. Three of them were $Al_{0.01}Ga_{0.99}As$ films with doping concentrations of 3.0×10^{18}, 4.7×10^{18}, and 7.1×10^{18} cm^{-3}, respectively. The other was $Al_{0.16}Ga_{0.84}As$ film doped to 4.7×10^{18} cm^{-3}. The second set of samples was C-doped 280-nm-thick GaAs epitaxial films with doping concentrations of 1.3×10^{19}, 2.4×10^{19}, and 4.7×10^{19} cm^{-3} grown on a 350-μm-thick semi-insulating GaAs substrate. The Al fraction, and the Be- and C-doping concentrations of the samples were analyzed by secondary-ion-mass spectrometry (SIMS). Carbon was used as a dopant since it allows a high level of doping compared to beryllium. The FIR reflectance spectra of the samples were recorded using a Perkin–Elmer system 2000 Fourier transform infrared (FTIR) spectrometer in the frequency region of 1.5–15 THz (i.e., 200–20 μm or 50–500 cm^{-1}) at room temperature. These measurements (near normal incidence $\theta<10°$) were done with a resolution of 4 cm^{-1}. The illuminated area on the epilayers was about 4 mm in diameter.

III. RESULTS AND DISCUSSION

A. Data analysis

The reflectance of the single film on the substrate can be calculated by Snell's law and Maxwell's equations considering the film to be isotropic.[18] The matrix method is used since it enables easy calculation of reflectance for an arbitrary number of parallel and isotropic layers. Suppose the complex refractive index of the film is $\tilde{n}_f$, vacuum is unity, and the substrate is $\tilde{n}_s$, respectively. The resultant matrix C_r is described by the following product form:

$$C_r = C_{vf}C_fC_{fs}. \tag{1}$$

Here, C_{vf} is the interface matrix between vacuum and film

$$C_{vf} = \frac{1}{2\tilde{n}_f}\begin{bmatrix} (\tilde{n}_f+1) & (\tilde{n}_f-1) \\ (\tilde{n}_f-1) & (\tilde{n}_f+1) \end{bmatrix}, \tag{2}$$

and C_f is the propagation matrix for the film

$$C_f = \begin{bmatrix} \exp(i2\pi\tilde{n}_f d/\lambda) & 0 \\ 0 & \exp(-i2\pi\tilde{n}_f d/\lambda) \end{bmatrix}, \tag{3}$$

where λ is the incident wavelength, d is the film thickness, and C_{fs} is the interface matrix between film and substrate

$$C_{fs} = \frac{1}{2\tilde{n}_s}\begin{bmatrix} (\tilde{n}_s+\tilde{n}_f) & (\tilde{n}_s-\tilde{n}_f) \\ (\tilde{n}_s-\tilde{n}_f) & (\tilde{n}_s+\tilde{n}_f) \end{bmatrix}, \tag{4}$$

the reflectance can be readily obtained from

$$R = \left|\frac{C_{r2,1}}{C_{r2,2}}\right|^2. \tag{5}$$

For doped semiconductor materials, the terahertz dielectric response functions are expressed by a multioscillator for the optical phonons and the Drude model for free carrier or plasma response. The dielectric function ($\varepsilon=\varepsilon_1+i\varepsilon_2$) of the $Al_xGa_{1-x}As$ films is written as

$$\varepsilon(\omega) = \varepsilon_\infty - \frac{\varepsilon_\infty\omega_p^2}{\omega(\omega+i\gamma)} + \sum_{k=1}^{2}\frac{S_k\omega_{\mathrm{TO},k}^2}{\omega_{\mathrm{TO},k}^2-\omega^2-i\omega\Gamma_k}. \tag{6}$$

Here, ε_∞ is the high-frequency dielectric constant, ω_p is the plasma frequency, γ is the free-carrier damping constant (related to the scattering time by $\tau=1/2\pi c\gamma$), $\omega_{\mathrm{TO},k}$ is the transverse-optical (TO) phonon frequency, S_k is the TO phonon strength, Γ_k is the damping parameter of the TO phonon, and ω is the frequency of the incident light. The plasma frequency ω_p of free carriers with effective mass m^* and carrier concentration n_p is given by the following equation:

$$\omega_p = \sqrt{\frac{n_p e^2}{\varepsilon_o\varepsilon_\infty m^*}}. \tag{7}$$

Here, e is the electron charge, ε_o is the vacuum permittivity. Only the n_p/m^* ratio is determined from the plasma frequency. It is noted that a single-Lorentz oscillator is used for the $Al_xGa_{1-x}As$ ($x\leqslant0.01$) films because the GaAs-like TO phonon was observed while the AlAs-like TO phonon was very weak in the measured terahertz frequency region. However, two Lorentz oscillators must be considered for the $Al_{0.16}Ga_{0.84}As$ film because the GaAs-like and AlAs-like TO phonons were both visible from the experimental reflectance spectra. In modeling the experimental data, two steps were considered. First, all the parameters in Eq. (6) were used as free parameters and determined using a least-square fitting program. It was found that the GaAs-like (about 268 cm^{-1}) and AlAs-like (about 358 cm^{-1}) TO phonons for all the $Al_xGa_{1-x}As$ films had almost the same frequency as the values reported in Refs. 19 and 20. In the second step, all the Lorentz parameters obtained in the first step were fixed in order to reduce the model parameter correlation, and only the Drude parameters (ω_p and γ) were calculated. It is reasonable that the TO phonon frequency is nearly the same in all samples because the doping concentration only slightly affects the phonon frequency.[21] The reflectance spectrum for the $Al_{0.16}Ga_{0.84}As$ film was well reproduced using the two-oscillator model, as shown in Fig. 1(c), which demonstrates the validity of the Drude model in the low-frequency region for the second step in the calculations.

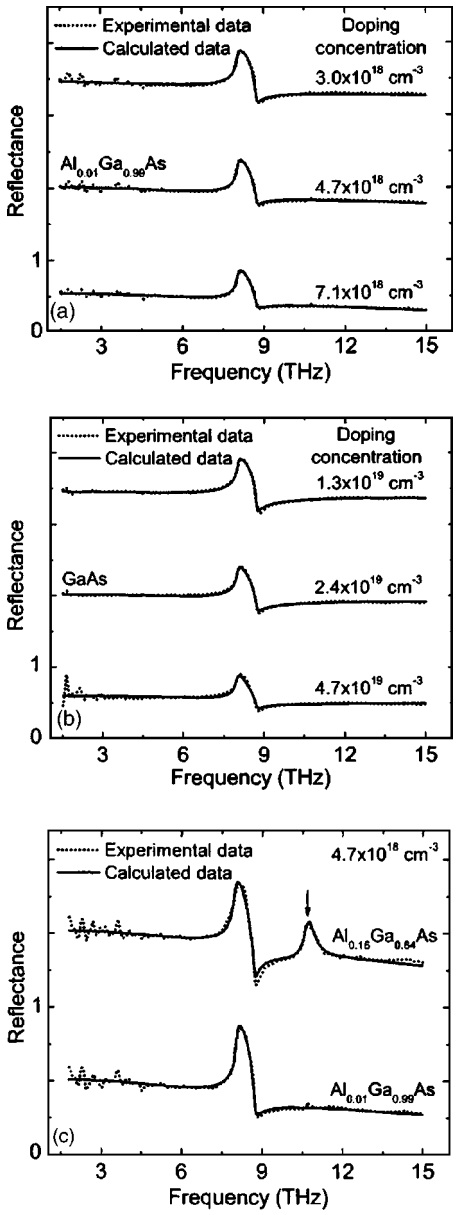

FIG. 1. Measured (dotted lines) and calculated (solid lines) terahertz reflectance spectra of (a) $Al_{0.01}Ga_{0.99}As$ films with different doping concentrations, (b) GaAs films with different doping concentrations, and (c) $Al_xGa_{1-x}As$ films with different Al fractions. The arrow in (c) shows the AlAs-like TO phonon frequency. For clarity, each spectrum is successively shifted by 1.5 in the vertical direction.

The reflectance R was calculated using the three-phase model (air/$Al_xGa_{1-x}As$ film/GaAs substrate). The interface layer between the film and substrate was neglected because of its small effects. The optical constants of the GaAs substrate were also calculated using Eq. (6) with the parameter values in Ref. 17. By adjusting the Drude parameter values of Eq. (6) to fit the experimental spectra to theoretical spectra, the best parameter values for the epitaxial films were determined. The optical constants ($\tilde{n}_f = n + i\kappa$) were calculated from

$$\tilde{n}_f(\omega) = \sqrt{\varepsilon(\omega)}. \tag{8}$$

The experimental (dotted lines) and calculated spectra (solid lines) for the $Al_xGa_{1-x}As$ epilayers are shown in Fig. 1. No mathematical smoothing has been performed on the experimental data. The agreement improves as the doping concentration increases. The multiple reflections in the substrate were not considered in the calculations. The GaAs-like TO phonon was observed near 8.1 THz (i.e., 268 cm^{-1}) for all epilayers. The AlAs-like TO phonon was clearly visible near 10.7 THz (i.e., 358 cm^{-1}) for the $Al_{0.16}Ga_{0.84}As$ film, as shown in Fig. 1(c). There are some interference peaks in the low-frequency (long wavelength) region since the substrate is polished on both sides. In the low-frequency region
($\leqslant$5 THz), the reflectance shows a slowly increasing trend with decreasing frequency. Generally, the free-carrier behavior plays an important role beyond the TO phonon frequency region. This implies that the Drude model can reasonably explain the absorption of the heavily doped $Al_xGa_{1-x}As$ films.

TABLE I. The parameter values for two sets of p-type $Al_xGa_{1-x}As$ epitaxial films. The plasma frequency ω_p and the free-carrier damping constant γ were obtained from the fitting calculations. Beryllium (Be) is the dopant for the $Al_xGa_{1-x}As$ ($\geqslant$0.01) films, and carbon (C) is the dopant for the GaAs films. The 90% confidence limit are given with ($\pm$).

Samples	Doping Concentration N_p ($\times 10^{18}$ cm^{-3})	ω_p (cm^{-1})	γ (cm^{-1})	$\frac{n_p}{N_p}\frac{m_N^*}{m_n^a}$
$Al_{0.01}Ga_{0.99}As$	3.0	279±4	367±17	1.59
$Al_{0.01}Ga_{0.99}As$	4.7	331±3	339±10	1.34
$Al_{0.16}Ga_{0.84}As$	4.7	364±6	373±18	1.60
$Al_{0.01}Ga_{0.99}As$	7.1	392±2	377±8	1.17
GaAs	13	572±10	547±27	1.53
GaAs	24	658±7	398±13	1.05
GaAs	47	832±13	341±17	0.90

The Drude parameter values used in the calculations are listed in Table I. The plasma frequency (correspondingly the free-carrier concentration) increases with the doping concentration. Note that the doping concentration of the $Al_{0.01}Ga_{0.99}As$ and $Al_{0.16}Ga_{0.84}As$ films is 4.7×10^{18} cm^{-3} and their plasma frequencies are slightly different. However, the value is located between that of the samples with doping concentrations of 3.0×10^{18} and 7.1×10^{18} cm^{-3}. The discrepancy could be due to the effects of the Al fraction and the AlAs-like TO phonon. Based on the previous discussions, the n_p/m^* value is determined from the plasma frequency since the effective mass m^* may deviate from the intrinsic bulk material value. Therefore, the ratio contains the effect of the doping concentration on the effective mass. The ratios are close to unity and show a decreasing trend with the doping concentration. This indicates that the hole concentration is in agreement with the doping concentration and the hole effective mass increases with the doping concentration.[17] For the GaAs films with the two highest doping concentrations, the ratios are 1.05 and 0.90, respectively. This implies that the hole concentration is almost equal to the doping concentration and has the smallest discrepancy in the hole effective mass. For the GaAs film with the doping concentration of 4.7×10^{19} cm^{-3}, this ratio (0.90) is slightly less than unity indicating that the hole effective mass is the largest for the

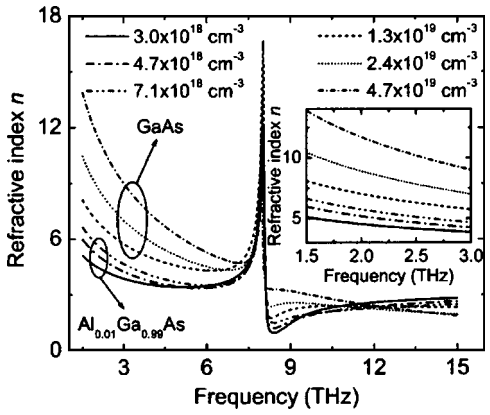

FIG. 2. The variation of the refractive index for the $Al_xGa_{1-x}As$ films with different doping concentrations in the frequency region of 1.5–15 THz. The upper three curves are for C-doped GaAs films and the lower three curves are for Be-doped $Al_{0.01}Ga_{0.99}As$ films. The inset shows an enlargement of the 1.5–3-THz frequency region of the refractive indices.

highest doping concentration. The dependence of the hole effective mass on the doping concentration is complicated since the contributions from the heavy and light holes are different. The Drude model considers their average effects and a good agreement was obtained by adjusting only two parameters. With respect to the doping concentrations up to 10^{19} cm^{-3} for the $Al_xGa_{1-x}As$ films, the present results confirm the conclusion that the deviation from the Drude model increases as the doping level decreases.[8]

B. Effects of doping concentration on optical constants

The calculated optical constants n and κ are shown in Figs. 2 and 3, respectively. The inset in Fig. 2 shows the refractive indices of the $Al_xGa_{1-x}As$ films with different doping concentrations in the 1.5–3-THz frequency region. The refractive index increases with the doping concentration in the low-frequency region. However, there are differences between the values above and below 8.1 THz, which indicate that the TO phonon provides a large contribution to the refractive index in this frequency region. Isenberg and Warta reported similar refractive index increasing at long wavelengths for heavily doped silicon layers.[22] The extinction coefficient increases with the doping concentration in the entire frequency region. As shown in Figs. 2 and 3, the optical constants increase quickly with decreasing frequency, and the differences between the samples become very large in the low-frequency region ($\leqslant$5 THz). However, these differences are small beyond the TO phonon frequency. The optical constants of the $Al_xGa_{1-x}As$ ($x=0.01$ and 0.16) films with a doping concentration of 4.7×10^{18} cm^{-3} are shown in Fig. 4. The refractive index and the extinction coefficient increase slightly with the Al fraction in the low-frequency region. It should be noted that the AlAs-like TO phonon is neglected in the mode for the $Al_{0.01}Ga_{0.99}As$ films. This results in the second peak (10.7 THz) of the optical constants for the $Al_{0.16}Ga_{0.84}As$ film. It indicates that the Al fraction can also affect the terahertz optical properties (free-carrier absorption behavior) since the doping concentration is the same. By using the Kane model, Metzger *et al.* calculated the shift of the Fermi level relative to the conduction-band valley of GaAs and InAs with different carrier concentrations.[23,24] The results indicate that the shift of the Fermi level increases with the carrier concentration. Although the shift is not large for the lightly doped samples, it increases quickly with heavily doped samples. For the epilayers with doping concentrations of $10^{18}-10^{19}$ cm^{-3} in this work, the theoretically calculated Fermi level shifts approximately from 0.2 to 0.7 eV. This shift is large compared to the terahertz photon energy. The Fermi-level shift can induce a redistribution of the free carriers above the conduction band if the effective mass changes slightly for different doping concentrations or Al fractions. The situation becomes much more complicated in p-type $Al_xGa_{1-x}As$ materials since the free holes occupy the heavy-hole and light-hole energy bands. This energy shift is expected to affect the two band distributions and the occupying possibility of heavy and light holes strongly. Moreover, both the intervalence band and the free-carrier transition dominate the terahertz optical properties of the $Al_xGa_{1-x}As$ films due to lower photon energy, contributing to the optical constants. The interaction between the tera-

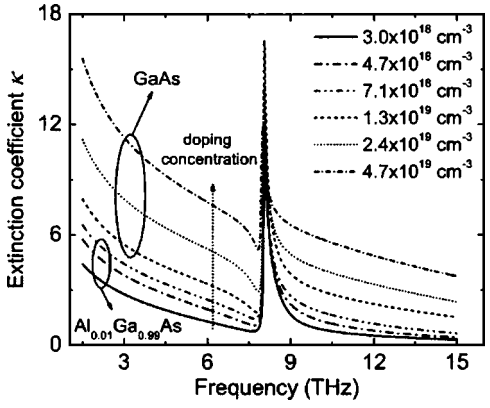

FIG. 3. The variation of the extinction coefficient for the $Al_xGa_{1-x}As$ films with different doping concentrations in the frequency region of 1.5–15 THz. The upper three curves are for C-doped GaAs films, and the lower three curves are for Be-doped $Al_{0.01}Ga_{0.99}As$ films.

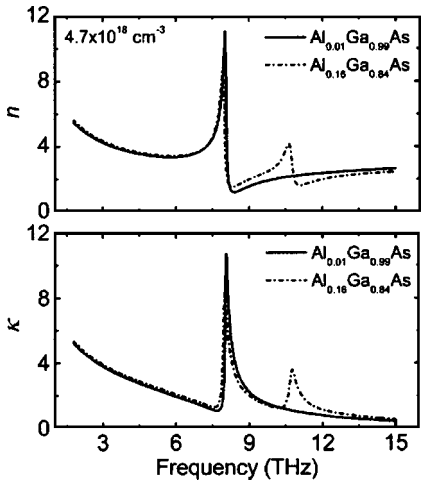

FIG. 4. The optical constants for Be-doped $Al_xGa_{1-x}As$ films with different Al fractions. The doping concentration is 4.7×10^{18} cm^{-3}. The AlAs-like TO phonon was observed at 10.7 THz for the $Al_{0.16}Ga_{0.84}As$ film.

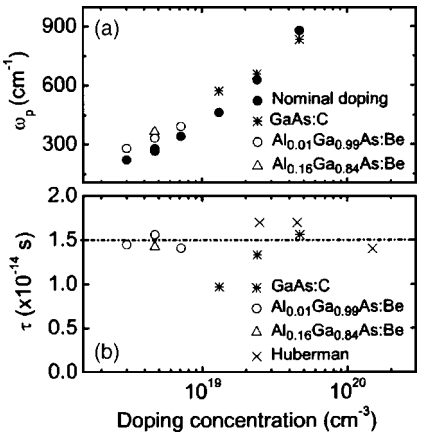

FIG. 5. (a) Plasma frequency ω_p and (b) scattering time τ were calculated from the experimental reflectance spectra with different doping concentrations. The values from Ref. 25 are also shown. The dash line indicates the average value of the scattering times obtained in the present work.

hertz radiation and the free carrier may change with the free hole distributions for *p*-type materials. Therefore, the dielectric response to the terahertz radiation is different and the optical constants vary with the doping concentration for the $Al_xGa_{1-x}As$ epilayers.

C. Effects of doping concentration on Drude parameters

For *p*-type $Al_xGa_{1-x}As$ materials, the free carriers are holes which populate two different bands, the heavy-hole and the light-hole bands, to different extents in *k* space.[17] The Drude model considers the simplest approximation for the contribution to the terahertz dielectric functions of the plasma. From the present results, it can be concluded that the approximation is reasonable. For clarity, the calculated results compared with the nominal doping concentration, and the damping constants (i.e., scattering times) are shown in Figs. 5(a) and 5(b), respectively. The calculated plasma frequencies are close to the theoretical results, indicating that the calculated results can be reasonably used to obtain the plasma frequencies. The difference may be due to the presence of a near-face depletion layer, which was not considered in the three-phase model. The calculated reflectance spectra using a four-phase model, which contains the depletion layer on the $Al_xGa_{1-x}As$ film layer, did not change the values listed in Table I within the confidence limits. The average free-carrier scattering time for the samples is close to 1.39×10^{-14} s. Huberman *et al.* reported that the scattering time varies from 1.7×10^{-14} to 1.4×10^{-14} s as the doping concentration increases from 2.5×10^{19} to 1.5×10^{20} cm^{-3}.[25] The present results are also close to those data except for a *p*-type GaAs epilayer with the doping concentration of 1.3×10^{19} cm^{-3}, which has a lower scattering time. Note that the scattering time in the Drude model is independent of frequency and it represents the average value for all terahertz frequencies. The different doping concentrations can affect the free hole transport properties due to changing free hole density. Also the Al fractions destroy GaAs-lattice long-range order, inducing the scattering time variations. The competition between the two effects appears for the

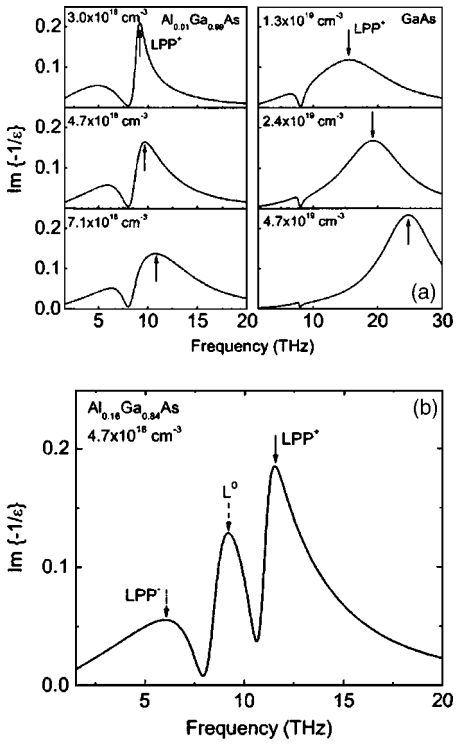

FIG. 6. Spectral density function Im$\{-1/\varepsilon\}$ of (a) the $Al_xGa_{1-x}As$ ($x\leqslant0.01$) films and (b) $Al_{0.16}Ga_{0.84}As$ film with different doping concentrations. The arrows indicate the LPP-coupled modes.

$Al_xGa_{1-x}As$ films with different Al fractions and doping concentrations. These perturbations are not considered in the simplest Drude theory.[25] In addition, the fluctuation of the scattering time may be attributed to the optical model because the GaAs substrates are polished on both sides and the model neglects the multiple reflections in the substrate. The large hole effective mass and different dopants also may affect the scattering time.[26]

D. Longitudinal-optical phonon plasmon coupled modes

The longitudinal-optical phonon plasmon (LPP)-coupled modes of *p*-type GaAs films have been investigated for different dopants and doping concentrations using Raman-scattering or infrared reflectance spectra.[13–15,21] The nature of the LPP-coupled modes in ternary alloy systems is complicated as a consequence of the two-mode behavior of their zone-center optical modes.[27] If the doping concentration is not high ($\leqslant10^{19}$ cm^{-3}), the LPP$^-$ mode is close to the GaAs-like TO phonon frequency and the LPP$^+$ mode shifts from the AlAs-like LO to the plasmonlike when plasmon frequency is beyond the AlAs-like LO frequency. On the other hand, the peak L^0 should change from the GaAs-like LO to the AlAs-like TO with increasing doping concentration (Note that the GaAs-like phonon is separated from the AlAs-like phonon, which occupies the high-frequency parts.[28]) Figures 6(a) and 6(b) show the LPP-coupled modes obtained from the spectral density function Im$\{-1/\varepsilon\}$ for the $Al_xGa_{1-x}As$ ($x\leqslant0.01$) films and the $Al_{0.16}Ga_{0.84}As$ film, respectively. A single mode was observed near the GaAs-like TO phonon for the $Al_{0.01}Ga_{0.99}As$ and GaAs films, as listed in Table II. The

TABLE II. The LPP-coupled mode values for two sets of *p*-type $Al_xGa_{1-x}As$ epitaxial films were determined from Figs. 6(a) and 6(b).

Samples	Dopant	Doping concentration N_p ($\times 10^{18}$ cm^{-3})	LPP$^+$ (cm^{-1})		
$Al_{0.01}Ga_{0.99}As$	Be	3.0		306	
$Al_{0.01}Ga_{0.99}As$	Be	4.7		323	
$Al_{0.01}Ga_{0.99}As$	Be	7.1		360	
GaAs	C	13		517	
GaAs	C	24		641	
GaAs	C	47		823	
			LPP$^-$	L^0	LPP$^+$
$Al_{0.16}Ga_{0.84}As$	Be	4.7	201	306	384

broadening of the LPP-coupled modes is due to the higher damping constant, higher hole effective mass, and lower hole mobility.[16] In particular, the lower branch (255 cm^{-1}) of the GaAs epilayer with the highest doping concentration is close to the GaAs-like TO phonon frequency (268 cm^{-1}). The upper LPP$^+$ modes increase with the doping concentration and show the transition from phononlike to plasmonlike behavior.[15] The LPP$^-$ mode for *p*-type GaAs film with a doping concentration of 2.0×10^{19} cm^{-3} has been observed at a frequency of 266 cm^{-1} by Yuasa and Ishii,[21] which is similar to the present work. It should be noted that the uncoupled plasma frequency is larger than the GaAs-like TO phonon frequency for all epilayers. Also, the upper LPP$^+$ mode values are close to the uncoupled plasma frequency (ω_p in Table I) and become broader with increasing doping concentration. This indicates the ability to derive the LPP-coupled modes from the infrared reflectance spectra. The LPP-coupled modes of the $Al_{0.16}Ga_{0.84}As$ film with the doping concentration of 4.7×10^{18} cm^{-3} are shown in Fig. 6(b) and listed in Table II. One can clearly identify the three coupled modes, which are labeled as LPP$^-$, L^0, and LPP$^+$, from the spectral density function Im$\{-1/\varepsilon\}$ and these are similar to the modes reported in Ref. 21 for the $Al_{0.2}Ga_{0.8}As$ film obtained using Raman scattering. The corresponding frequencies are 6.2 THz (201 cm^{-1}), 9.2 THz (306 cm^{-1}), and 11.5 THz (384 cm^{-1}). Therefore, these three features of the $Al_{0.16}Ga_{0.84}As$ film in this work are in agreement with the above analysis. It should be noted that the L^0 value (306 cm^{-1}) is close to the GaAs-like LO frequency (292 cm^{-1}).

E. Relationship between doping concentration and absorption coefficient

The free-carrier absorption (FCA) coefficient has a simple quadratic dependence on wavelength; however, the theory is only valid at frequencies beyond about 20 THz.[22,29] Although the measured frequency region in the present work is below the above value, a similar phenomenon was observed for the $Al_{0.01}Ga_{0.99}As$ films in the high-frequency region, but not for the GaAs films as their doping concentrations are very high. However, the absorption coefficient decreases slightly with decreasing frequency in the low-frequency region ($\leqslant$3 THz). It is clear from the Drude parameters in Eq. (6) that ω is similar to γ at lower frequencies. The saturation of the absorption coefficient is not observed up to 1.5 THz in the present work.

The calculated absorption coefficients ($\alpha=4\pi\kappa/\lambda$) are shown in Fig. 7. The absorption coefficient is one of the important factors in terahertz detectors. Previous literatures have reported the free-carrier absorption for *p*-type GaAs with low doping concentrations (up to 10^{18} cm^{-3}) only in a relatively high-frequency range ($\geqslant$15 THz).[25,26] Similar to the extinction coefficient, the absorption coefficient increases with the doping concentration. The absorption coefficient is about 7.5×10^3 cm^{-1} for the *p*-type GaAs layer with the doping concentration of 1.3×10^{19} cm^{-3} at 3.75 THz (80 μm). The shift of the absorption coefficient at 3.75 THz, which is the threshold frequency for some of the designed terahertz detectors, relative to the doping concentration is shown in Fig. 8. The terahertz absorption coefficient of the $Al_{0.01}Ga_{0.99}As$ and GaAs epilayers can be fitted to the following empirical relationship:

$$\alpha_{3.75} = 2.3\times10^{-6}N_p^{0.50}, \tag{9}$$

where the effect of the small Al fraction is negligible. Here, N_p is the doping concentration in cm^{-3}. Recently, Ray *et al.* reported a relationship of $\alpha_{3.75}=3.5\times10^{-8}N_p^{0.60}$ for doped silicon films at the same frequency.[9] While the reported absorption coefficient in the above literature is from the experimental transmittance and reflectance measurements, the present work focuses only on the reflectance data. Based on

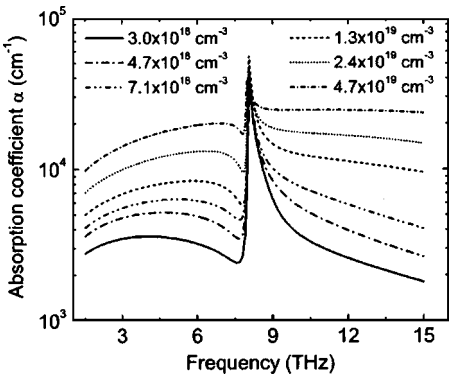

FIG. 7. The variation of the absorption coefficient for the $Al_{0.01}Ga_{0.99}As$ and GaAs films with different doping concentrations in the frequency region of 1.5–15 THz.

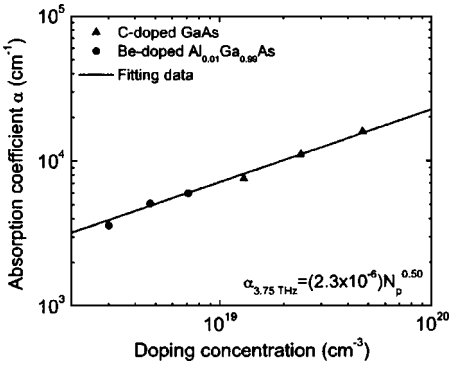

FIG. 8. The sublinear relationship between the doping concentration and the absorption coefficient of the $Al_{0.01}Ga_{0.99}As$ and GaAs films at 3.75 THz (80 μm).

Eq. (9), increasing the doping concentration can improve the performance of terahertz detectors. However, the absorption coefficient approaches a constant as the doping concentration increases at low frequencies. It is expected that the absorption coefficient approaches the values of metallic materials because the doping concentration is close to or above Mott transition concentration. The sublinear relationship between the terahertz absorption coefficient and the doping concentration needs to be further studied in order to improve the performance of terahertz detectors.

IV. CONCLUSIONS

In conclusion, optical constants of *p*-type $Al_xGa_{1-x}As$ ($x=0$, 0.01 and 0.16) epitaxial films with different beryllium and carbon doping concentrations have been investigated in the terahertz frequency region from 1.5 to 15 THz. With the three-phase model (air/film/substrate) and the classical Lorentz–Drude model, the experimental reflectance spectra can be fitted to derive the optical constants. The results indicate that the refractive index and extinction coefficient increase with the hole concentration. The calculated plasma frequency is close to the theoretical result. The average free-carrier scattering time is about 1.39×10^{-14} s. The LPP-coupled modes of the $Al_xGa_{1-x}As$ films were investigated. The upper LPP^+ mode increases with the doping concentration and shows a transition from phononlike to plasmonlike behavior. Three LPP-coupled modes were observed for the $Al_{0.16}Ga_{0.84}As$ film. The corresponding frequencies are 6.2, 9.2, and 11.5 THz, respectively. The absorption coefficient for the $Al_xGa_{1-x}As$ films decreases slightly with the increasing frequency. A sublinear relationship between the absorption coefficient and the doping concentration was found at 3.75 THz.

ACKNOWLEDGMENTS

The work was supported in part by the U.S. NSF under Grant No. ECS-0140434 and U.S. Department of Energy under Grant No. DE-FG03. The authors would like to acknowledge Dr. H. C. Liu for many fruitful discussions.

[1] S. G. Matsik, M. B. M. Rinzan, A. G. U. Perera, H. C. Liu, Z. R. Wasilewski, and M. Buchanan, Appl. Phys. Lett. **82**, 139 (2003).
[2] D. G. Esaev, S. G. Matsik, M. B. M. Rinzan, A. G. U. Perera, H. C. Liu, and M. Buchanan, J. Appl. Phys. **93**, 1879 (2003).
[3] H. C. Liu, C. Y. Song, A. J. Spring Thorpe, and J. C. Cao, Appl. Phys. Lett. **84**, 4068 (2004).
[4] M. Graf, G. Scalari, D. Hofstetter, J. Faist, H. Beere, E. Linfield, D. Ritchie, and G. Davies, Appl. Phys. Lett. **84**, 475 (2004).
[5] A. L. Korotkov, A. G. U. Perera, W. Z. Shen, J. Herfort, K. H. Ploog, W. J. Schaff, and H. C. Liu, J. Appl. Phys. **89**, 3295 (2001).
[6] P. R. Griffths and J. de Haseth, *Fourier Transform Infrared Spectroscopy* (Wiley, New York, 1986).
[7] M. van Exter and D. Grischkowsky, Phys. Rev. B **41**, 12140 (1990).
[8] P. G. Huggard, J. A. Cluff, G. P. Moore, C. J. Shaw, S. R. Andrews, S. R. Keiding, E. H. Linfield, and D. A. Ritchie, J. Appl. Phys. **87**, 2382 (2000).
[9] S. K. Ray, T. N. Adam, R. T. Troeger, J. Kolodzey, G. Looney, and A. Rosen, J. Appl. Phys. **95**, 5301 (2004).
[10] T. Tsuchiya, S. Ozaki, and S. Adachi, J. Phys.: Condens. Matter **15**, 3717 (2003).
[11] S. Adachi, *Optical Constants of Crystalline, Amorphous Semiconductors: Numerical Data and Graphical Information* (Kluwer Academic Publishers, Boston, 1999).
[12] H. R. Chandrasekhar and A. K. Ramdas, Phys. Rev. B **21**, 1511 (1980).
[13] K. Wan and J. F. Young, Phys. Rev. B **41**, 10772 (1990).
[14] A. Mlayah, R. Carles, G. Landa, E. Bedel, and A. Muñoz-Yagüe, J. Appl. Phys. **69**, 4064 (1991).
[15] R. Fukasawa, K. Sakai, and S. Perkowitz, Jpn. J. Appl. Phys., Part 1 **36**, 5543 (1997).
[16] M. Seon, M. Holtz, W. M. Duncan, and T. S. Kim, J. Appl. Phys. **85**, 7224 (1999).
[17] W. Songprakob, R. Zallen, W. K. Liu, and K. L. Bacher, Phys. Rev. B **62**, 4501 (2000).
[18] O. S. Heaven, *Optical Properties of Thin Solid Films* (Dover, New York, 1991).
[19] S. Adachi, *GaAs and Related Materials: Bulk Semiconducting and Superlattice Properties* (World Scientific, Singapore, 1994).
[20] D. J. Lockwood and Z. R. Wasilewski, Phys. Rev. B **70**, 155202 (2004).
[21] T. Yuasa and M. Ishii, Phys. Rev. B **35**, 3962 (1987).
[22] J. Isenberg and W. Warta, Appl. Phys. Lett. **84**, 2265 (2004).
[23] W. K. Metzger, M. W. Wanlass, L. M. Gedvilas, J. C. Verley, J. J. Carapella, and R. K. Ahrenkiel, J. Appl. Phys. **92**, 3524 (2002).
[24] E. O. Kane, J. Phys. Chem. Solids **1**, 249 (1957).
[25] M. L. Huberman, A. Ksendzov, A. Larsson, R. Terhune, and J. Maserjian, Phys. Rev. B **44**, 1128 (1991).
[26] R. Braunstein and E. O. Kane, J. Phys. Chem. Solids **23**, 1423 (1962).
[27] O. K. Kim and W. G. Spitzer, Phys. Rev. B **20**, 3258 (1979).
[28] J. Ibáñez, E. Tarhan, A. K. Ramdas, S. Hernández, R. Cuscó, L. Artús, M. R. Melloch, and M. Hopkinson, Phys. Rev. B **69**, 075314 (2004).
[29] D. K. Schroder, *Semiconductor Materials and Device Characterization* (Wiley, New York, 1990).